Supporting Information

Origin of size dependency in coherent-twin-propagation mediated tensile deformation of noble metal nanowires

Jong-Hyun Seo,[†,‡,∇] Harold S. Park,[§,∇] Youngdong Yoo,[‖] Tae-Yeon Seong,[‡] Ju Li,[¶]

Jae-Pyoung Ahn,[†,*], Bongsoo Kim,[‖,*] In-Suk Choi[⊥,*]

[†]Advanced Analysis Center, KIST, Seoul 130-650, Korea

[‡]Department of Materials Science and Engineering, Korea University, Seoul 136-701, Korea

[§]Department of Mechanical Engineering, Boston University, Boston, MA 02215, USA

[‖]Department of Chemistry, KAIST, Daejeon 305-701, Korea

[¶]Department of Nuclear Science and Engineering and Department of Materials Science and Engineering, Massachusetts Institute of Technology, Cambridge, MA 02139, USA

[⊥]High Temperature Energy Materials Research Center, KIST, Seoul 130-650, Korea

KEYWORDS: Nanowires, ultra-strong and ductile, twin propagation, size effect, surface energy

1. After experimentally acquiring the stress-strain curves, we performed a series of additional tensile test with the NW diameter of about 98 nm in the SEM while stopping the test at each deformation stage. Subsequently, we took the NWs at each stage in order to obtain structural details with TEM images in the insets of Figure 1.

Twin propagation and surface reorientation of the single crystalline Pd NW during stage II : The Figure S1 provides more detailed structural information of the inset of Stage 2. As shown in Figure S1 (a), the NW became tilted across the twin boundary. Selected area electron diffraction (SAED) patterns of the original and twinned regions (Figure S1 b,c,d) show that the twin formation reorients the lattice of the NW from <110> to <100>. The region (b) and (c) indicate single crystallinity of NW during the twin propagation while a concurrent axial reorientation from <110> to <100> is observed in region (c). The SAED patterns for the region (d) clearly shows the twin boundary structure.

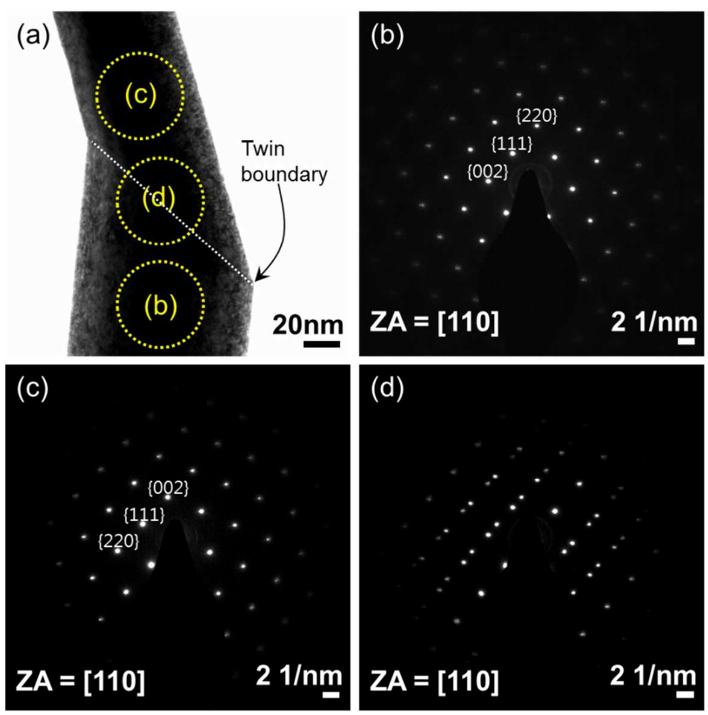

Figure S1: TEM observation at Stage 2 illustrating the geometrical changes that occur during the tensile stress-induced reorientation of the Pd NW from <110>{111} to <100>{100}. (a)

Bright field TEM image across the twin boundary (a) and (b,c) SAED patterns acquired from two yellow dotted circles denoted by (b) and (c) with a 180 nm aperture, the NW lattice is changed from an original <110>/(111) (b) to a twinned <100>/(100) (c). SAED pattern across the boundary from the circled area (d) shows a clear twin structure.

2. Derivation of surface energy differential model (equation 12): As shown in Figure S2, the tensile load induces a lattice reorientation which results in the complete geometrical transformation of the initially <110>{111} NW into a <100>{100} NW. The reorientation of the NW results in a change of the cross sectional geometry, from rhombic for the initially <110>/{111} NW to square for the <100>/{100} NW. In conjunction, the cross-sectional area decreases and the four bounding {111} surfaces of the initially rhombic <110>/{111} NW are reoriented to {100} surfaces.

The axial reorientation from <110> to <100> also results in a significant elongation of the NW, where the change in the NW dimensions can be summarized as

$$\mathrm{d} = \frac{2}{\sqrt{6}} \cdot \mathrm{d}_0,\ l = \sqrt{2} \cdot l_0 \quad \cdots\cdots\cdots(1)$$

where d_0 and d are the initial and final side lengths, respectively, and l_0 and l are the initial and final axial lengths of the <110>{111} and <100>{100} NWs, respectively. Because it is well-known that for metals undergoing plastic deformation, volume is preserved, we could confirm the volume conservation as

$$\mathrm{V}_0 = \frac{2\sqrt{2}}{3} \mathrm{d}_0{}^2 \cdot \mathrm{l}_0 \quad \cdots\cdots\cdots(2)$$

$$\mathrm{V} = \mathrm{d}^2\mathrm{l} = \left(\frac{2}{\sqrt{6}}\mathrm{d}_0\right)^2 \sqrt{2} \cdot \mathrm{l}_0 = \frac{2\sqrt{2}}{3} \mathrm{d}_0{}^2 \cdot \mathrm{l}_0 \quad \cdots\cdots\cdots(3)$$

Work must be done on the NW to propagate the twins that reorient the NW from <110>/{111} to <100>/{100}, and so we write the energetics related to twin propagation as

$$\Delta W = \Delta(\gamma S) + \Delta E_{elastic} + \Delta Q \quad \cdots\cdots\cdots\cdots\cdots\cdots\cdots (4)$$

where $\Delta(\gamma S)$ is the change in surface energy of the four surfaces of the NW due to the lattice reorientation, $\Delta E_{elastic}$ is the stored elastic energy and ΔQ is the energy dissipation due to the lattice friction, etc. The work done during the tensile testing of the NWs can be written as

$$\Delta W = F\Delta l \quad \cdots\cdots\cdots\cdots\cdots\cdots\cdots (5)$$

where F is the applied force along the NW axis during twin propagation, and Δl is the corresponding length change. Thus, we can calculate the applied force F by equating (4) and (5) in the following equation (6), where equations (4) and (5) are obtained from Li et al [ref. *1*]

$$F = \frac{\Delta(\gamma S)}{\Delta l} + \frac{\Delta E_{elastic}}{\Delta l} + \frac{\Delta Q}{\Delta l} \quad \cdots\cdots\cdots\cdots\cdots\cdots\cdots (6)$$

The elastically stored energy is relaxed during plastic deformation and the dissipation energy is also not a major contribution to the energetics of twin propagation in the NWs, as previously discussed by Li et al. [ref. 1] and Liang et al. [ref. 2]. Thus, we have assumed that the applied force can be written purely in terms of the surface energy difference $\Delta(\gamma S)$ as a result of the twin migration.

The total surface energies of the <110>{111} and <100>{100} NWs are written as

$$\gamma S_{<100>\{100\}\,NW} = \gamma_{100} \cdot 4l \cdot d \quad \cdots\cdots\cdots\cdots\cdots\cdots\cdots (7)$$

$$\gamma S_{<110>\{111\}\,\mathrm{NW}} = \gamma_{111} \cdot 4l_0 \cdot \mathrm{d}_0 = \gamma_{111} \cdot 4(\tfrac{1}{\sqrt{2}} l \cdot \tfrac{\sqrt{6}}{2}\mathrm{d}) = \gamma_{111} 4l \cdot \mathrm{d} \cdot \tfrac{\sqrt{3}}{2} \cdots\cdots\cdots\cdots (8)$$

where γ_{111} and γ_{100} are the surface energies for the {111} and {100} surfaces, respectively and S is the area of a bounding surface.

The surface energy difference after twin migration can be calculated as

$$\Delta(\gamma S) = \gamma S_{<100>\{100\}\,\mathrm{NW}} - \gamma S_{<110>\{111\}\,\mathrm{NW}}$$

$$= \gamma_{100} \cdot 4\mathrm{l} \cdot \mathrm{d} - \gamma_{111} 4l \cdot \mathrm{d} \cdot \frac{\sqrt{3}}{2}$$

$$= 4l \cdot \mathrm{d}\left(\gamma_{100} - \tfrac{\sqrt{3}}{2}\gamma_{111}\right) \cdots\cdots\cdots\cdots (9)$$

Therefore we can calculate the applied force along the <100> NW direction for twin propagation as

$$\mathrm{F}\Delta l = \Delta \mathrm{W} = \Delta(\gamma S)$$

The length change is $\Delta l = (l - l_0) = \frac{(\sqrt{2}-1)}{(\sqrt{2})} l$ so that

$$\mathrm{F} \cdot \frac{(\sqrt{2}-1)}{\sqrt{2}} \cdot l = 4\mathrm{d} \cdot l\left(\gamma_{100} - \frac{\sqrt{3}}{2}\gamma_{111}\right)$$

$$\mathrm{F} = 4\mathrm{d}\frac{\sqrt{2}}{(\sqrt{2}-1)}\left(\gamma_{100} - \tfrac{\sqrt{3}}{2}\gamma_{111}\right) \cdots\cdots\cdots\cdots (10)$$

Then, the stress along the reoriented <100> wire can be written as

$$\sigma = \frac{\mathrm{F}}{\mathrm{A}_{100}} = \frac{\mathrm{F}}{\mathrm{d}^2} = \frac{4\sqrt{2}}{(\sqrt{2}-1)}\left(\gamma_{100} - \tfrac{\sqrt{3}}{2}\gamma_{111}\right)\frac{1}{\mathrm{d}} \cdots\cdots\cdots\cdots (11)$$

where $\mathrm{A}_{100}$is the cross-sectional area of the reoriented <100> NW with <100>.

Because we measured the diameter d_0 of the <110>/{111} NWs in our experiment before twin migration, we replace d with d_0 by inserting $d = \frac{2}{\sqrt{6}} \cdot d_0$

$$\sigma = \frac{4\sqrt{3}}{(\sqrt{2}-1)}\left(\gamma_{100} - \frac{\sqrt{3}}{2}\gamma_{111}\right)\frac{1}{d_0} \quad \cdots\cdots\cdots\cdots\cdots\cdots\cdots(12)$$

Our model given in Equation (12) was plotted with our experimental data in the Figure 5 in the main text. As seen in the main text, the model slightly underpredicts the twin propagation stress, though the overall trend is captured. We believe that one reason for this is because the normal stress in the <100> direction may be lower than the apparent stress due to grip constraints at the NW ends.

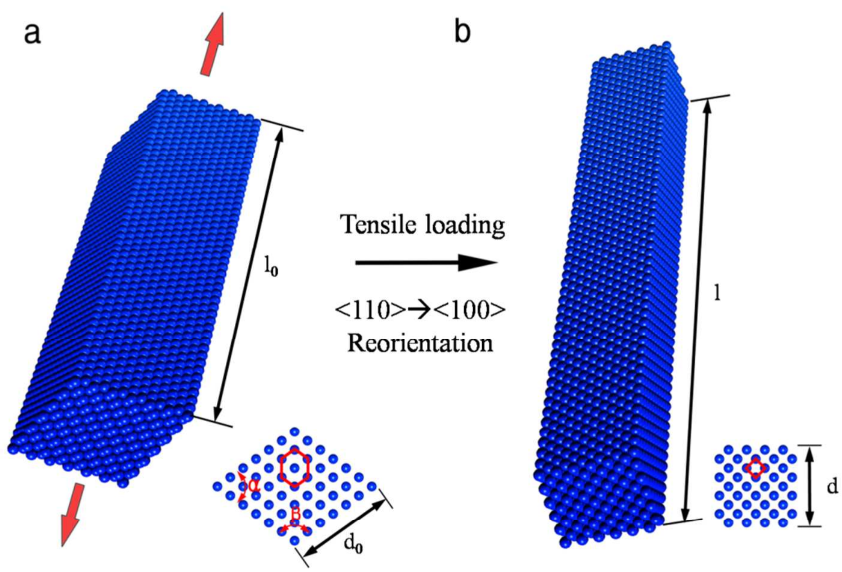

Figure S2. Schematic illustrating the geometrical changes that occur during the tensile stress-induced reorientation of the NW from <110>{111} to <100>{100}.

3. Size dependence of yield strength: Unlike the twin migration stress, the size dependence of the yield stress does not overlap for the Pd, AuPd and Au NWs as shown in the Figure S3.

This is because the stacking fault energy is the dominant factor controlling the dislocation nucleation process that governs yielding. Because the stacking fault energy of Pd is about twice that of Au, the yield stress of Pd is higher than Au [ref. 3], with the yield stress of AuPd lying in between pure Pd and pure Au.

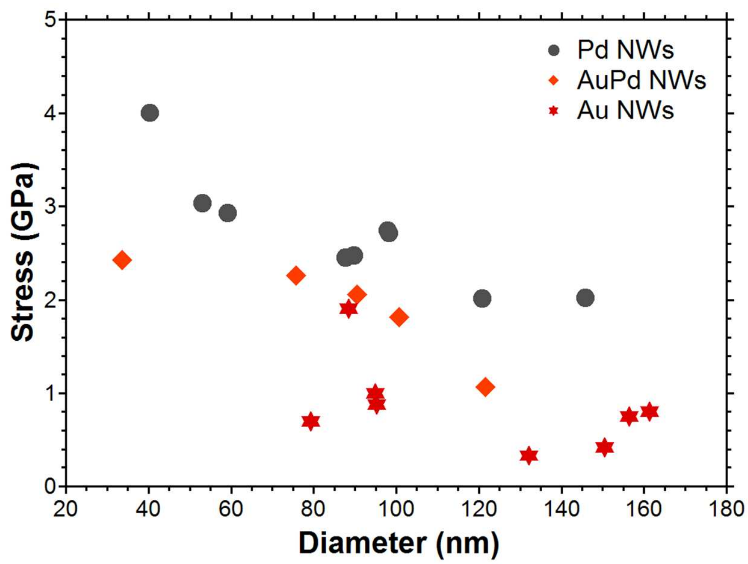

Figure S3: Size-dependence of the yield stress for the <110>/{111} Pd, AuPd, Au NWs.

4. Calculation of Cross sectional area: For stress calculation, we divided the force by the rhombic cross-sectional area of the NW. Figure S4 (a) shows that the original NWs with <110>/(111) have a rhombic cross-section. We measured the diagonal of the NWs from the side view of the SEM image as in Figure S4 (b) and calculated the area assuming the rhombic area as schematically shown in Figure S4 (c).

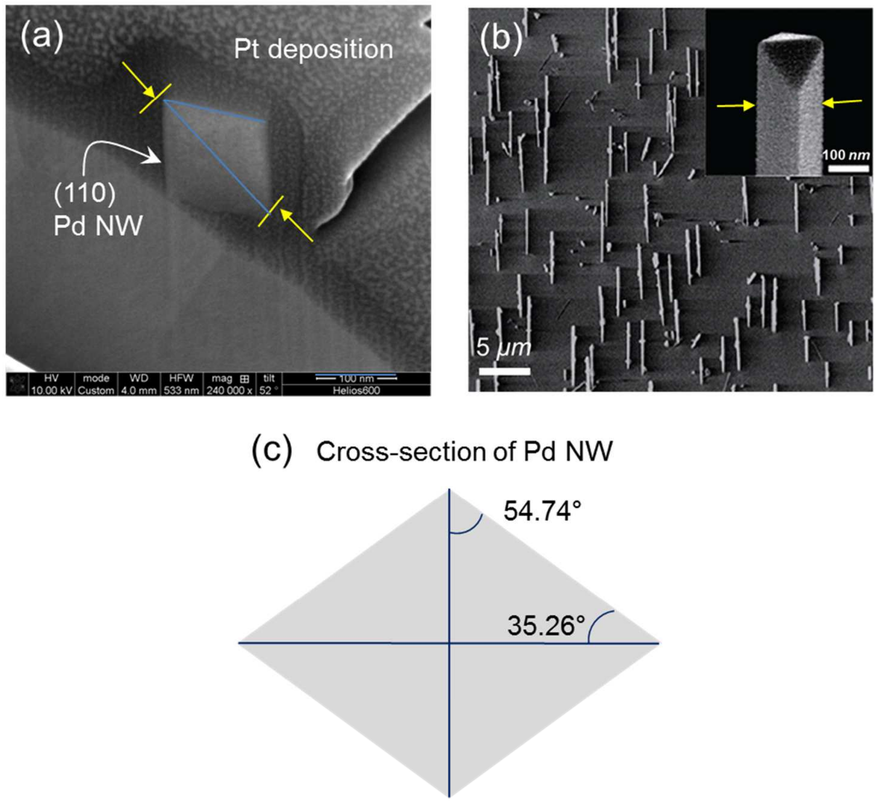

Figure S4: (a) SEM image of the cross-sectional area of a representative Pd NW showing a rhombic shape with <110>{111}. (b) 45° tilted SEM images of vertically grown Pd NWs on a c-cut sapphire substrate. The inset is a magnified image showing clear facets of the rhombic NW. (c) Schematic of the rhombic cross-section of the Pd NWs based on Figure S4 (a). We used this schematic to calculate the cross-sectional area.

5. Possible reason for deviation between the measured and predicted twin migration stress in Figure 5 :

1) Underestimation of the cross sectional area may lead to overestimation of the measured twin propagation stress. As mentioned before, we measured the width of the NWs from the side view of the SEM image. As shown in Figure S5, the diagonal can be underestimated though we tried to calibrate the angle of the view point. However, since we employed the NWs all grown in the same vertical direction, the diagonals were measured in a consistent way so the underestimation should be consistent as well. Hence, the trend and the exponent value should be valid.

2) Possible misalignment of the NW and geometrical tilt during twin propagation may also overestimate the measured stress as well.

3) The dissipation energy (about 100 MPa) was not included in the surface energy differential model as mentioned in the manuscript. This can underestimate the predicted twin migration stress [ref. 1].

4) The predicted twin propagation is quite sensitive to the surface energy values in Eq. (1) in the main text. We used values for surface energy that were obtained from ab initio calculations, but the values can vary depending on the simulation scheme [ref. 3]. Thus, the inaccuracy of the surface energy for (111) and (100) planes we used may deviate and underestimate the predicted twin propagation stress.

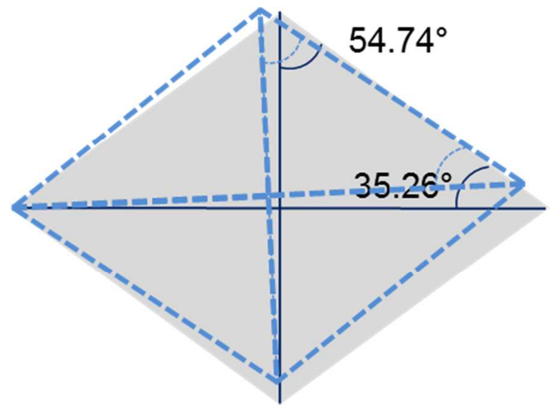

Figure S5: Schematic illustration of possible underestimation of the rhombic cross-section of the Pd NWs.

References

[1] S. Li, X. Ding, J. Li, X. Ren, J. Sun, E. Ma, *Nano Lett.* **10**, 1774 (2010).

[2] W. Liang, D.J. Srolovitz, M. Zhou, *Journal of the Mechanics and Physics of Solids* **55**, 1729 (2007).

[3] J. Wan, Y.L. Fan, D.W. Gong, S.G. Shen, X.Q. Fan, *Modelling and Simulation in Materials Science and Engineering* **7**, 189 (1999).

6. Supplementary movies of *in-situ* tensile testing

We provide two different tensile tests showing in movie S1 and movie S2 to resolve the issue that may arise because of the AFM cantilever. The movie S1 shows the tensile test without the AFM cantilever. The movie S2 shows a tensile test with the AFM cantilever.

Movie S1:

The tensile test without an AFM cantilever showing the twin propagation of a <110> Pd NW.

Movie S2:

The tensile test of a <100> Pd NW with an AFM cantilever, separated from the <110> region remained after the twin propagation was completed.

Both of them showed apparently the same mechanical deformation of the NWs including long range ordered twin propagation behavior. The test in movie S1 is undoubtedly a displacement control controlled by the piezo response of the nanomanipulator. The test in movie S2 may not be an ideal displacement control since the AFM cantilever is attached to the manipulator. However, considering the much higher stiffness of the cantilever and the manipulator than that of the NW, we believe that our AFM cantilever based tensile test is more likely displacement control test by controlling the piezo movement of the manipulator. Furthermore, a significant load drop is explicitly observed, which indicated the displacement control.